

Conducting Polyaniline/Iron Oxide Composite: A Novel Adsorbent for the Removal of Amido Black 10B

Rais Ahmad* and Rajeev Kumar

Environmental Research Laboratory, Department of Applied Chemistry, Aligarh Muslim University, Aligarh, 202002, India

In this work, a polyaniline/iron oxide (PANIIO) composite was prepared and evaluated for its amido black 10B (AB10B) dye adsorption characteristics from aqueous solution. Adsorption equilibrium kinetic and thermodynamic experiments of AB10B onto PANIIO were studied in a batch system. The effects of solution pH, initial dye concentration, contact time, and temperature on the adsorption capacity of PANIIO for AB10B have been investigated. The pseudofirst-order and pseudosecond-order kinetic models were used to describe the kinetic data. It was found that adsorption kinetics followed the pseudosecond-order kinetic model at all of the studied temperatures. The Langmuir and Freundlich adsorption models were used for the mathematical description of adsorption equilibrium data, and the best fit was obtained using the Freundlich isotherm with an R^2 value of 0.9948. The change of Gibbs energy, enthalpy, and entropy of adsorption was also evaluated for the adsorption of AB10B onto PANIIO.

1. Introduction

Synthetic dye stuffs are extensively used as coloring agents in the textile, paper, leather, gasoline, pharmaceutical, and food industries. Their discharge into the hydrosphere presents a significant source of pollution due to both their visibility even at very low concentrations and recalcitrance, giving undesirable color to the water, reducing sunlight penetration, and resisting photochemical and biological attack, and their degradation products being toxic or even mutagenic.^{1,2} Synthetic dyes usually have a complex aromatic molecular structure which possibly comes from coal-tar-based hydrocarbons such as benzene, naphthalene, anthracene, toluene, xylene, and so forth. The complex aromatic molecular structures of dyes make them more stable and more difficult to biodegrade.^{3,4} The main technologies employed for the treatment of dye-containing effluents are chemical precipitation, adsorption, ion exchange, biodegradation, membrane filtration, coagulation, flocculation, and so forth. However, only adsorption is the most versatile and widely used because other methods require high capital investment and have low efficiency.^{5,6}

Recently, composite materials have been emerging as alternative adsorbents for the scavenging of dyes from wastewater. They have unusual hybrid mechanical, thermal, physical, and chemical properties. They also have a large surface area, which makes the composite materials as good adsorbents as the parent materials.⁷

Polyaniline (PANI), a well-known conducting polymer, has been subjected to extensive use in lightweight battery electrodes, sensors, electromagnetic shielding devices, and anticorrosion coatings.⁸ PANI has been studied most extensively since it has a unique doping mechanism, excellent physicochemical properties, and good stability and its raw material can be obtained easily.^{9,10} PANI is a selective adsorbent for the anionic dyes. These characteristics are mainly due to the interaction between the negatively charged anion of the dye and the positively

charged PANI backbone.¹¹ Therefore, PANI has much potential as an inexpensive and effective adsorbent for almost all anionic dyes, because of its innate cationic nature.

The objective of the current study was to improve the selective capabilities of PANI for anionic dyes. To accomplish this endeavor, PANI was doped with iron oxide because iron oxides also have a selective adsorptive nature for the anionic dyes.^{12,13} In this work adsorption properties of polyaniline/iron oxide (PANIIO) for the removal of amido black 10B (AB10B) from aqueous solution was investigated. Kinetics, equilibrium isotherms, and thermodynamic parameters were evaluated to find the adsorption mechanism.

2. Materials and Methods

Aniline, dodecyl pyridinium bromide, and AB10B of analytical grade were purchased from the Central Drug House, India. Potassium persulfonate and ferrous sulfate was supplied by the Loba Chemico-Indo Austral Co. Ltd. and Qualigenus Fine Chemical, India, respectively. A stock solution of dye was prepared by dissolving the appropriate amount of AB10B in double-distilled water.

2.1. Synthesis of Iron Oxide. The iron oxide was synthesized by a coprecipitation method.¹³ A portion of 20 g of $\text{FeSO}_4 \cdot 7\text{H}_2\text{O}$ was dissolved in 100 mL of distilled water, and 50 mL of 5.0 M NaOH was added. The reaction mixture was stirred for 24 h. The precipitate was heated at 80 °C and sonicated for 1 h. The precipitated iron oxide was filtered out and washed thoroughly with distilled water and then dried at 100 °C.

2.2. Synthesis of Polyaniline/Iron Oxide Composite. PANIIO was prepared by the reported method.⁷ The PANIIO composite was prepared by the chemical oxidative polymerization of aniline in the presence of iron oxide. A portion of 8 g of iron oxide was mixed with acidic solution (0.1 M HCl) of 20 mL of 0.1 M aniline. To this 0.5 g of dodecyl pyridinium bromide was added and stirred for 30 min. The oxidant potassium persulfonate (0.1 M) was added drop by drop keeping the temperature at 4 °C with vigorous stirring for 8 h. The

* Corresponding author address. E-mail: rais45@rediffmail.com. Phone: +91-9997063442. Fax: +91-0571-2400528.

resulting precipitate was washed with methanol, acetone, and distilled water and dried at 80 °C.

2.3. Selectivity Study. The primary adsorption study was performed on both anionic (AB10B, alizarin red S, congo red) and cationic (methylene blue, crystal violet, malachite green) dyes. However, the PANIIO composite did not show any adsorption ability for cationic dyes. Therefore, the anionic AB10B dye was selected as a model adsorbate to study the adsorption potential of the synthesized PANIIO composite.

2.4. Batch Adsorption Studies. 2.4.1. Kinetic Experiments.

Batch kinetic experiments were performed by mixing 0.015 g of adsorbent to each 20 mL of dye solution of 50 mg·L⁻¹ concentration at (30, 40, and 50) °C, respectively. A series of such conical flasks were then shaken at a constant speed of 80 rpm in a water bath shaker, and samples were collected at different time intervals. Then the concentration of AB10B in the supernatant solution was analyzed using a double beam UV–visible spectrophotometer (Elico SL 164) at a wavelength of maximum absorbance (618 nm). The equilibrium adsorption capacity of PANIIO for AB10B was calculated from the relationship:

$$q_e = (C_0 - C_e)V/M \quad (1)$$

where q_e is the equilibrium adsorption capacity (mg·g⁻¹), C_e is the dye concentration (mg·L⁻¹) at equilibrium, V is the volume (L) of solution, and M is the weight (g) of adsorbent.

2.4.2. Equilibrium Experiments. The effect of the initial dye concentration was determined by placing 0.015 g of the adsorbent in 20 mL of dye solution of different initial concentrations [(30 to 80) mg·L⁻¹] for 180 min at 30 °C. The concentration of AB10B left in the supernatant solution was determined by spectrophotometry.

2.4.3. Effect of pH on AB10B Adsorption. The influence of pH on the AB10B adsorption was studied over the pH range from 2 to 10. The pH was adjusted using dilute NaOH and HCl solutions. In this study, 20 mL of dye solution of 50 mg·L⁻¹ was agitated with 0.015 g of adsorbent for 180 min at 30 °C. The concentration of AB10B left in the supernatant solution was analyzed by spectrophotometry.

2.5. Desorption and Regeneration Studies. Desorption studies were performed in batch with 0.1 M HCl, 0.1 M CH₃COOH, 0.1 M NaCl, 0.1 M NaOH, and 99 % CH₃OH. Initially, 0.015 g of adsorbent was agitated with the dye of concentration of 50 mg·L⁻¹ for 180 min. After the equilibrium time, the dye saturated adsorbent was separated, washed with distilled water to remove the traces of unadsorbed dye, and agitated with 20 mL of eluent for 180 min. The amount of the dye released into the eluent solution was determined by:

$$\% \text{ desorption} = (C_e/C_a)100 \quad (2)$$

where C_a is the concentration of dye adsorbed on adsorbent, while C_e is the concentration of dye in the eluent solution after its desorption from the adsorbent.

The regeneration study was performed by a column process. The column of dimensions 30 cm in length and 1 cm in internal diameter was packed with 0.1 g of PANIIO. Then the column was loaded with the dye solution of concentration 50 mg·L⁻¹ at the flow rate of 1 mL·min⁻¹. The column was operated until the effluent concentration matched the concentration of the loaded dye. After complete saturation of the adsorbent, distilled water was passed through the column to remove traces of unadsorbed dye. The 0.1 M NaOH was used as an eluent to regenerate the adsorbent.

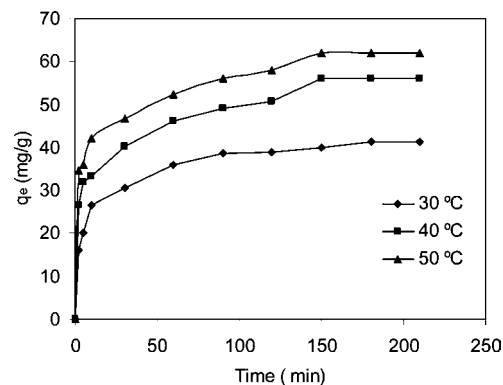


Figure 1. Effect of contact time on AB10B adsorption.

3. Results and Discussion

3.1. Effect of Contact Time and Kinetics. The adsorption of AB10B from aqueous solution onto PANIIO as a function of contact time and temperature is shown in Figure 1. The adsorption of AB10B increases with increasing contact time and temperature. Figure 1 shows that the adsorption of AB10B consisted of two phases: (i) an initial rapid phase where adsorption was fast and contributed significantly to the equilibrium uptake (external surface adsorption) and (ii) a slower phase whose contribution to the total dye adsorption was relatively small (internal surface adsorption). From Figure 1, it is clear that the adsorption capacity increased with an increase in temperature. This indicated that a higher temperature favored AB10B removal and the adsorption was endothermic in nature.

Adsorption kinetics data were simulated with a pseudofirst-order model and pseudosecond-order model. The linear pseudofirst-order and pseudosecond-order equations were:

$$\log(q_e - q_t) = \log q_e - k_1 t / 2.303 \quad (3)$$

$$t/q_t = (1/k_2 q_e^2) + t/q_e \quad (4)$$

where q_e and q_t are the amounts of dye adsorbed at equilibrium and time t (mg·g⁻¹), respectively. k_1 and k_2 are the rate constants for the pseudofirst-order and pseudosecond-order kinetics models.

The experimental data in Figure 1 have been applied to the pseudofirst-order and pseudosecond-order rate equation kinetics at (30, 40, and 50) °C, respectively, expressed as the equations below:

For the pseudofirst-order model:

$$\log(q_e - q_t) = 1.3193 - 0.0048t \quad q_e = 20.43 \quad R^2 = 0.9692 \quad (5)$$

$$\log(q_e - q_t) = 1.4156 - 0.0061t \quad q_e = 26.03 \quad R^2 = 0.9781 \quad (6)$$

$$\log(q_e - q_t) = 1.1570 - 0.0070t \quad q_e = 26.04 \quad R^2 = 0.9913 \quad (7)$$

and for the pseudosecond-order model

$$t/q_t = 0.0238t + 0.1695 \quad q_e = 42.01 \quad R^2 = 0.9980 \quad (8)$$

$$t/q_t = 0.0810t + 0.1307 \quad q_e = 55.55 \quad R^2 = 0.9910 \quad (9)$$

$$t/q_t = 0.0162t + 0.0967 \quad q_e = 61.72 \quad R^2 = 0.9946 \quad (10)$$

From the above equations, it is evident that the experimental data showed a good compliance with the pseudosecond-order

model. The values of coefficient of determination for the pseudosecond-order equations were higher than the pseudofirst-order equations at all of the experimental temperatures, and on the other hand, the calculated q_e values are close to the experimental q_e data for the pseudosecond-order model than the calculated values of the pseudofirst-order model. These observations suggested that the overall rate of AB10B adsorption was controlled by pseudosecond-order kinetics.

3.2. Thermodynamic Studies. The thermodynamic parameters, standard Gibbs free energy change (ΔG°), enthalpy change (ΔH°), and entropy change (ΔS°) were estimated to evaluate the feasibility of the adsorption process by the following equations:

$$\Delta G^\circ = RT \ln K_c \quad (11)$$

$$\ln K_c = -(\Delta H^\circ/RT) + \Delta S^\circ/R \quad (12)$$

where K_c is the distribution coefficient for the adsorption, R is the universal gas constant ($8.314 \text{ J}\cdot\text{mol}^{-1}\cdot\text{K}^{-1}$), and T is the absolute temperature (K). On the basis of the experimental data in Figure 1, at different temperatures, the van't Hoff equation of AB10B adsorption onto PANIIO was given as follows:

$$\ln K_c = 30.022 - 1076.9/T \quad R^2 = 0.999 \quad (13)$$

The negative ΔG° values, (1.233, 4.15, and $7.389 \text{ kJ}\cdot\text{mol}^{-1}$ for (303, 313, and 323) K, respectively, increased with temperature, indicating the feasibility and spontaneity of the adsorption process of AB10B onto PANIIO. The positive value of ΔH° ($8.953 \text{ kJ}\cdot\text{mol}^{-1}$) confirmed the endothermic nature of the adsorption process, while the positive value of ΔS° ($249.6 \text{ J}\cdot\text{mol}^{-1}\cdot\text{K}^{-1}$) revealed the increase in randomness at the solid-solution interface during the adsorption process.

3.3. Effect of Concentration and Adsorption Isotherms. The dye adsorptive capacity of PANIIO at equilibrium increased from (27 to 56) $\text{mg}\cdot\text{g}^{-1}$ when increasing the initial concentration from (30 to 80) $\text{mg}\cdot\text{L}^{-1}$. This was obvious because a more efficient utilization of the adsorption capacities of the adsorbent was expected due to a greater driving force by a higher concentration gradient pressure.¹⁴

Langmuir and Freundlich adsorption isotherms were used to fit the experimental data. The linear Langmuir and Freundlich equations were

$$C_e/q_e = (1/bq_{\max}) + C_e/q_{\max} \quad (14)$$

$$\ln q_e = \ln K_F + 1/n \ln C_e \quad (15)$$

where C_e is the equilibrium concentration of the dye solution ($\text{mg}\cdot\text{L}^{-1}$), q_e is the amount of dye adsorbed at equilibrium ($\text{mg}\cdot\text{g}^{-1}$), and q_{\max} and b are the Langmuir constants related to the monolayer adsorption capacity ($\text{mg}\cdot\text{g}^{-1}$) and surface energy ($\text{mg}\cdot\text{L}^{-1}$), respectively. K_F is the Freundlich constant ($\text{mg}\cdot\text{g}^{-1}$) ($\text{mg}\cdot\text{L}^{-1}$)^{1/n}, and $1/n$ is the heterogeneity factor.

From the experimental data, the Langmuir and Freundlich equations were, respectively, expressed as the equations below:

$$C_e/q_e = 0.0068C_e + 0.8918 \quad R^2 = 0.9695 \quad (16)$$

$$\ln q_e = 0.7888 \ln C_e + 0.036 \quad R^2 = 0.9948 \quad (17)$$

From eqs 16 and 17, the Freundlich model was found to precisely fit the equilibrium data as evidenced by a higher correlation coefficient of determination value than the Langmuir

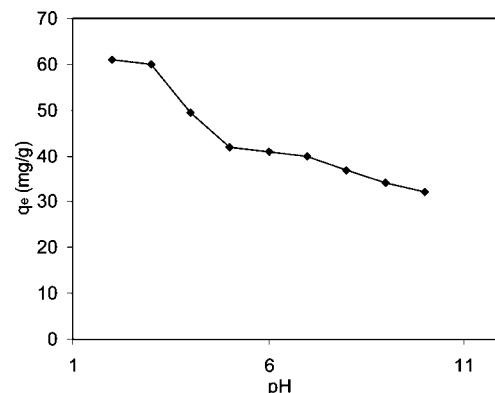


Figure 2. Effect of pH on AB10B adsorption.

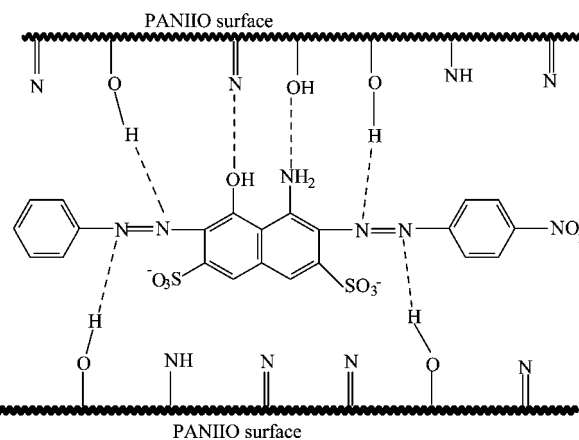


Figure 3. Proposed mechanism for the adsorption of AB10B onto the PANIIO surface. =N, -NH, and -OH representing the functional groups present on the PANIIO composite.

model. It is also clear from eq 17 that the value of the Freundlich exponent n (1.269) was greater than one, illustrating that AB10B was favorably adsorbed onto PANIIO.¹⁵⁻¹⁷

3.4. Effect of pH. The effect of dye solution pH onto AB10B adsorption was studied in the pH range 2 to 10. The results indicate that the maximum uptake of AB10B takes place at pH 2.0 as shown in Figure 2. This behavior can be explained on the basis of change in surface charge of the PANIIO composite. At lower pH, the H^+ ion concentration in the system increases, and the surface of PANIIO acquires a positive charge by adsorbing H^+ ions. Positively charged surface sites on PANIIO favored the adsorption of the anionic dye molecules due to electrostatic interaction, leading to maximum dye adsorption. As the pH of the system increases, the number of negatively charged sites increases by absorbing OH^- ions. As the PANIIO surface is negatively charged at high pH, a significantly high electrostatic repulsion exists between the negatively charged surface of PANIIO and the anionic dye molecules, causing the decrease in dye adsorption. Similar results were reported for the adsorption of anionic fluoride ions onto PANI/alumina composite⁷ and anionic dyes onto doped PANI.^{11,18}

3.5. Desorption and Regeneration. As is evident from the pH studies that an acidic medium favors the adsorption most, hence no desorption was achieved with 0.1 M HCl and 0.1 M CH_3COOH . The desorption percentage of AB10B from PANIIO was 94 % for 0.1 M NaOH, 38 % for 99 % CH_3OH , and 8 % with 0.1 M NaCl. The higher desorption of dye with 0.1 M NaOH was likely due to the high basicity of 0.1 M NaOH as compared to 99 % CH_3OH and 0.1 M NaCl.

The regeneration of PANIIO for AB10B adsorption was tested by performing five cycles of adsorption/desorption.

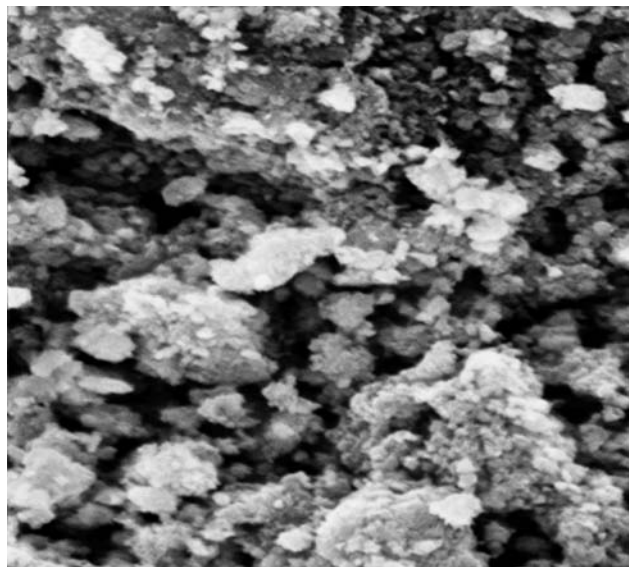


Figure 4. SEM image of PANIIO.

Column regeneration was carried out using 0.1 M NaOH. Only 30 mL of eluent was enough for complete desorption of the dye from the saturated adsorbent. The breakthrough and exhaustive capacities were (40, 35, 35, 35, and 35) $\text{mg}\cdot\text{g}^{-1}$ and (135, 115, 110, 110, and 110) $\text{mg}\cdot\text{g}^{-1}$ during the first, second, third, fourth, and fifth cycles, respectively.

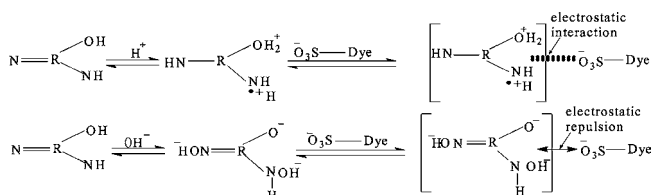
3.6. Adsorption Mechanism. There are many factors that may influence the adsorption of the dye such as charge and structure of dye, adsorbent surface properties, hydrophobic and hydrophilic nature, hydrogen bonding, electrostatic interaction, steric effect, and van der Waals forces, and so forth. The interaction between AB10B and PANIIO can be explained by the following process.

Hydrophobic–hydrophobic interaction exists between the hydrophobic part of the dye molecule and the hydrophobic

regions of adsorbent. In aqueous solution, nonpolar molecules or groups have a tendency to associate. This tendency, governed mainly by entropy, is called hydrophobic interaction.¹⁹

Hydrogen bonding interactions are possible between nitrogen and oxygen containing functional groups on the dye molecule and adsorbent surface. The amine, imine, and hydroxyl groups of the adsorbent form a hydrogen bond with the azo, hydroxyl, and amine groups of dyes as shown in Figure 3.

Electrostatic interaction between the anionic sulfonic groups of the dye and positively charged amine, imine, and hydroxyl groups of the adsorbent. At low pH (< 4), nitrogen atoms, mainly on the imine group, which are relatively easier to get protonated than the amine group,²⁰ interact quickly with the sulfonic group of the dye by electrostatic forces. The adsorption behavior of the dye in acidic and basic media can be shown as follows:



where R is used to indicate the surface of adsorbent containing =N, –NH groups of PANI, and the –OH group of iron oxide.

The energy released during the adsorption process compensates for the entropy loss of adsorbed molecules. The stronger the force, the more energy is released. The energy release by different forces during adsorption is unequal²¹ and ranges from van der Waals forces of (4 to 10) $\text{kJ}\cdot\text{mol}^{-1}$, hydrophobic bond forces of about 5 $\text{kJ}\cdot\text{mol}^{-1}$, hydrogen bond forces of (2 to 40) $\text{kJ}\cdot\text{mol}^{-1}$, coordination exchange of about 40 $\text{kJ}\cdot\text{mol}^{-1}$, dipole bond forces of (2 to 29) $\text{kJ}\cdot\text{mol}^{-1}$, and chemical bond forces of > 60 $\text{kJ}\cdot\text{mol}^{-1}$. In this study, the enthalpy change for AB10B adsorption was 8.953 $\text{kJ}\cdot\text{mol}^{-1}$, suggesting that all types of

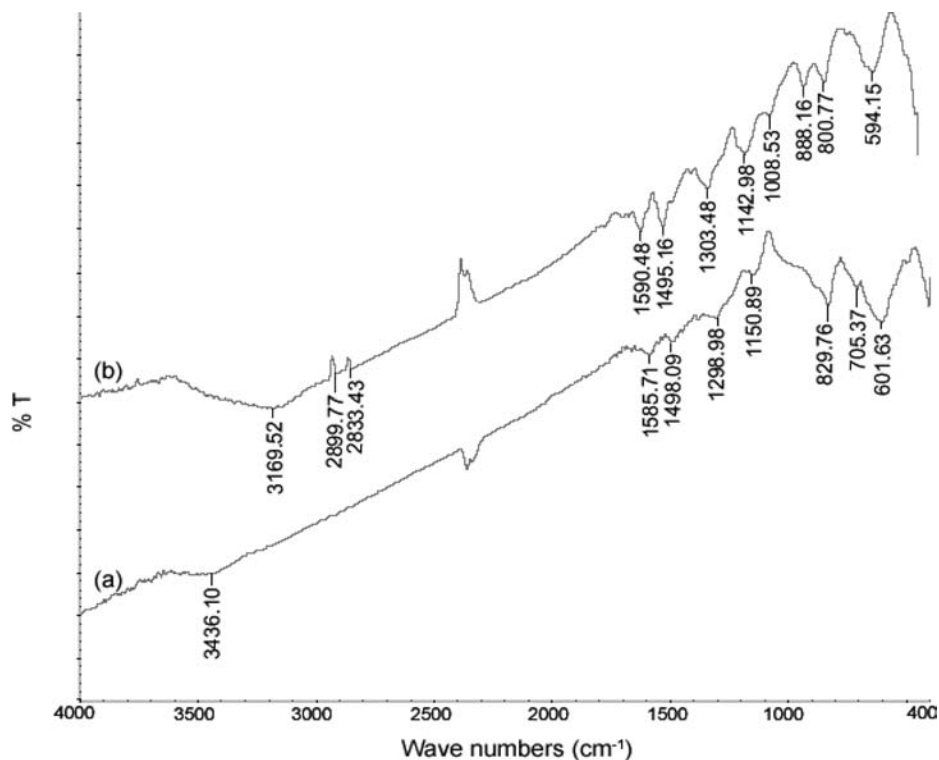


Figure 5. FTIR spectra of PANIIO composite (a) before adsorption and (b) after adsorption.

forces were involved except for coordination exchange and chemical bond forces.

3.7. Surface Morphology and FTIR Analysis. The scanning electron microscopy (SEM) image of PANIIO is shown in Figure 4. It can be seen from the figure that the surface is irregular and porous, which provides a good platform for AB10B adsorption.

The Fourier transform infrared (FTIR) spectra of PANIIO before adsorption (a) and after adsorption (b) are shown in Figure 5. The major changes are the following: the absorption band at 3436 cm^{-1} (Figure 5a), corresponding to the stretching vibration of —N—H , diminish after adsorption of the dye, and the appearance of a new absorption band at 1008 cm^{-1} , attributed to the S=O stretching of the dye (Figure 5b). The absorption bands at $(1585\text{ and }1498)\text{ cm}^{-1}$ can be assigned to the quinonoid ring and the benzenoid ring, respectively.²² Bands at $(1298\text{ and }1150)\text{ cm}^{-1}$ are due to C—N bending and in-plane bending of the C—H bond. The appearance of the C—H out-of-plane bending vibrational band of the 1,4-ring at 834 cm^{-1} suggests that a head-to-tail configuration is taken by PANI prepared in the current reaction system.^{23,24} The peaks observed between $(400\text{ and }700)\text{ cm}^{-1}$ correspond to Fe—O bonding of iron oxide.

4. Conclusion

PANIIO composites showed considerable potential for the removal of the anionic dye AB10B from aqueous solution. The adsorption takes place by the complexation between the amine, imine, and hydroxyl group of composite material and the azo, hydroxyl, and sulfonic groups of dye molecules. The adsorption capacity of PANIIO for AB10B decreased with increasing pH but increased with increasing temperature. The adsorption process of the AB10B dye on PANIIO followed pseudosecond-order kinetics and the Freundlich isotherm model.

Literature Cited

- Hastie, J.; Bejan, D.; Teutli-Leon, M.; Bunce, N. Electrochemical methods for degradation of orange II (Sodium 4-(2-Hydroxy-1-naphthylazo)benzenesulfonate). *J. Ind. Eng. Chem. Res.* **2006**, *45*, 4898–4904.
- Van der Zee, F. P.; Villaverde, S. Combined anaerobic-aerobic treatment of azo dyes, A short review of bioreactor studies. *Water Res.* **2005**, *39*, 1425–1440.
- Seshadri, S.; Bishop, P. L.; Agha, A. M. Anaerobic/aerobic treatment of selected azo dyes in wastewater. *Waste Manage.* **1994**, *15*, 127–137.
- Renmin, G.; Yingzhi, S.; Jian, C.; Huijun, L.; Chao, Y. Effect of chemical modification on dye adsorption capacity of peanut hull. *Dyes Pigm.* **2005**, *67*, 175–181.
- Aksu, Z.; Tezer, S. Equilibrium and kinetics modeling of biosorption of remazol black B by *rhizopus arrhizus* in a batch system: effect of temperature. *Process Biochem.* **2000**, *36*, 431–439.
- Walker, G. M.; Hansen, L.; Hana, J. A.; Allen, S. J. Kinetics of a reactive dye adsorption onto dolomite sorbent. *Water Res.* **2003**, *37*, 2081–2089.
- Karthikeyan, M.; Kumar, K. K. S.; Elango, K. P. Conducting polymer/alumina composites as viable adsorbents for the removal of fluoride ions from aqueous solution. *J. Fluorine Chem.* **2009**, *130*, 894–901.
- Shimano, J. Y.; MacDiarmid, A. G. Polyaniline, a dynamic block copolymer: Key to attaining its intrinsic conductivity. *Synth. Met.* **2001**, *123*, 251–262.
- Dhawan, S. K.; Singh, N.; Rodrigues, D. Electromagnetic shielding behaviour of conducting polyaniline composites. *Sci. Technol. Adv. Mater.* **2003**, *4*, 105–113.
- Sudha, J. D.; Sivakala, S.; Prasanth, R.; Reena, V. L.; Nair, P. R. Development of electromagnetic shielding materials from the conductive blends of polyaniline and polyaniline-clay nanocomposite-EVA: Preparation and properties. *Compos. Sci. Technol.* **2009**, *69*, 358–364.
- Mahanta, D.; Madras, G.; Radhakrishnan, S.; Patil, S. Adsorption and desorption kinetics of anionic dyes on doped polyaniline. *J. Phys. Chem. B* **2009**, *113*, 2293–2299.
- Stipp, S. L. S.; Hansen, M.; Kristensen, R.; Hochella, M. F.; Bennedsen, L.; Dideriksen, K.; Balic, Z. T.; Leonard, D.; Mathieu, H. J. Behaviour of Fe-oxides relevant to contaminant uptake in the environment. *Chem. Geol.* **2002**, *190*, 321–337.
- Pirillo, S.; Ferreira, M. L.; Rueda, E. H. Adsorption of alizarin, eriochrome blue black R, and fluorescein using different iron oxides as adsorbents. *Ind. Eng. Chem. Res.* **2007**, *46*, 8255–8263.
- Han, R.; Zhang, J.; Han, P.; Wang, Y.; Zhao, Z.; Tang, M. Study of equilibrium, kinetic and thermodynamic parameters about methylene blue adsorption onto natural zeolite. *Chem. Eng. J.* **2009**, *145*, 496–504.
- Namasivayam, C.; Jeyakumar, R.; Yamuna, R. T. Dye removal from wastewater by adsorption on waste Fe(III)/Cr(III) hydroxide. *Waste Manage.* **1994**, *14*, 643–648.
- Hameed, B. H.; Ahmad, A. A.; Aziz, A. Isotherms, kinetics and thermodynamics of acid dye adsorption on activated palm ash. *Chem. Eng. J.* **2007**, *133*, 195–203.
- Tunc, O.; Yanaci, H.; Aksu, Z. Potential use of cotton plant wastes for the removal of remazol black B reactive dye. *J. Hazard. Mater.* **2009**, *163*, 187–198.
- Mahanta, D.; Madras, G.; Radhakrishnan, S.; Patil, S. Adsorption of sulfonated dyes by polyaniline mmeraldine salt and its kinetics. *J. Phys. Chem. B* **2008**, *112*, 10153–10157.
- Muller-Dethlefs, K.; Hobza, P. Noncovalent interactions: a challenge for experiment and theory. *Chem. Rev.* **2000**, *100*, 143–167.
- Wang, J.; Deng, B.; Chen, H.; Wang, X. O.; Zheng, J. Z. Removal of aqueous Hg(II) by polyaniline: Sorption characteristics and mechanisms. *Environ. Sci. Technol.* **2009**, *43*, 5223–5228.
- Von Oepen, B.; Kordel, W.; Klein, W. Sorption of nonpolar and polar compounds to soils: processes, measurement and experience with the applicability of the modified OECD-guideline. *Chemosphere* **1991**, *22*, 285–304.
- Yang, P. C.; Du, J.; Peng, Q.; Qiao, R.; Chen, W.; Xu, C.; Shuai, Z.; Gao, M. Polyaniline/Fe₃O₄ nanoparticle composite: Synthesis and reaction mechanism. *J. Phys. Chem. B* **2009**, *113*, 5052–5058.
- Liu, W.; Kumar, J.; Tripathy, S.; Senecal, K. J.; Samuelson, L. Enzymatically synthesized conducting polyaniline. *J. Am. Chem. Soc.* **1999**, *121*, 71–78.
- Kang, E. T.; Neoh, K. G.; Tan, K. L. Polyaniline: A polymer with many interesting intrinsic redox states. *Prog. Polym. Sci.* **1998**, *23*, 277–324.

Received for review February 18, 2010. Accepted June 4, 2010.

JE1001686